



Cite this: DOI: 10.1039/c8nj01904e

Received 19th April 2018,  
Accepted 14th June 2018

DOI: 10.1039/c8nj01904e

rsc.li/njc

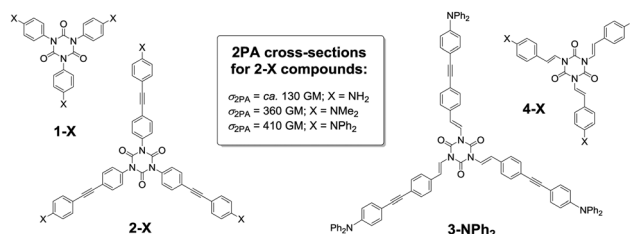
This contribution reports the synthesis of  $C_{87}H_{60}N_6O_3$  (**3-NPh<sub>2</sub>**), the tristyril analogue of the triphenylisocyanurate  $C_{81}H_{54}N_6O_3$  (**2-NPh<sub>2</sub>**) which was previously demonstrated to be an active two-photon absorber. Contrary to expectation, planarization and extension of the central  $\pi$ -system does not lead to a marked improvement of the two-photon absorption cross-section.

Since the seminal work of Cho,<sup>1,2</sup> planar octupolar molecules have attracted sustained interest for their two-photon absorption properties; this is because of the increasing attention given to this third-order nonlinear optical (NLO) property for applications in diverse fields ranging from microfabrication to bioimaging.<sup>2–5</sup> In this respect, we recently identified extended triazinane-2,4,6-triones such as **2-X** (Scheme 1), more commonly known as isocyanurates,<sup>6,7</sup> as exhibiting large hyperpolarizabilities for molecules of this size when functionalized by peripheral donor groups ( $X = NH_2$ ,  $NMe_2$ ,  $NPh_2$ ).<sup>8,9</sup>

As previously pointed out,<sup>9</sup> because of steric interactions between the oxygen atoms of the central ring and the *ortho* hydrogens of the peripheral phenyl groups of the molecule, the latter adopt a twisted conformation which results in a partial disruption of the  $\pi$ -manifold connecting the terminal electron-releasing groups to the central electron-deficient core. Given that the NLO properties are often strongly correlated with the spatial extension and good overlap of the conjugated  $\pi$ -manifold between donor and acceptor groups,<sup>10,11</sup> we logically wondered if the two-photon absorption (2PA) performance of such molecules

# Diphenylamino-substituted tristyril vs. triphenyl isocyanurates: improved conjugation has minimal impact on two-photon absorption†

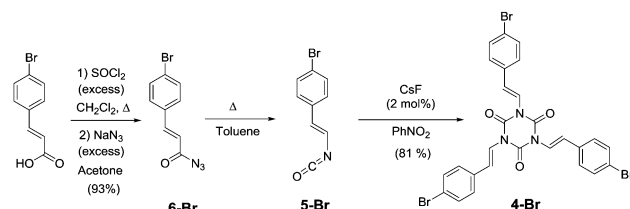
Amédée Triadon,<sup>ab</sup> Alphonsine Ngo Ndimba,<sup>ab</sup> Nicolas Richy,<sup>a</sup> Anissa Amar,<sup>c</sup> Abdou Boucekkine,<sup>id</sup> Thierry Roisnel,<sup>a</sup> Marie P. Cifuentes,<sup>b</sup> Mark G. Humphrey,<sup>id</sup> Mireille Blanchard-Desce,<sup>d</sup> Olivier Mongin<sup>id</sup>\*<sup>a</sup> and Frédéric Paul<sup>\*a</sup>



Scheme 1 Known (**1-X** and **2-X**;  $X = NH_2$ ,  $NMe_2$ ,  $NPh_2$ ) and targeted (**3-NPh<sub>2</sub>**, **4-X**;  $X = Br$ ) molecular structures. 2PA cross-sections are given for selected **2-X** compounds in Göppert-Mayer (GM) units.

could be improved by inserting 1,2-ethylene groups between the central isocyanurate core and the appended phenyl rings in the most active derivative **2-NPh<sub>2</sub>**. Such a chemical modification should planarize and slightly extend the  $\pi$ -manifold on each arm at the same time. To this aim, we targeted the derivative **3-NPh<sub>2</sub>**, using a synthetic approach requiring the preliminary isolation of **4-Br**. This molecule accessed following a workup inspired from that used by Mormann *et al.* to isolate its analogue **4-H** in a completely different context.<sup>12</sup>

Access to **4-Br** was achieved in one step by cyclotrimerization of the corresponding styryl isocyanate **5-Br**, itself generated from its acryloyl azide precursor **6-Br** using a Curtius reaction (Scheme 2) and engaged without purification in the cyclotrimerization step. The acryloyl azide precursor **6-Br** was isolated in good yields (93%), in two steps, from commercial 4-bromocinnamic acid and characterized by NMR.



Scheme 2 Synthesis of **4-Br**.

<sup>a</sup> Univ Rennes, CNRS, ISCR (Institut des Sciences Chimiques de Rennes), UMR 6226, F-35000 Rennes, France. E-mail: olivier.mongin@univ-rennes1.fr, frederic.paul@univ-rennes1.fr

<sup>b</sup> Research School of Chemistry, Australian National University, Canberra, ACT 2601, Australia. E-mail: Mark.Humphrey@anu.edu.au

<sup>c</sup> Département de Chimie, Faculté des Sciences, Université Mouloud Mammeri, 15000 Tizi-Ouzou and Faculté de chimie, USTHB, Alger, Algeria

<sup>d</sup> Univ. Bordeaux, ISM (CNRS-UMR 5255), 33405 Talence, France

† Electronic supplementary information (ESI) available. CCDC 1511480. For ESI and crystallographic data in CIF or other electronic format see DOI: 10.1039/c8nj01904e

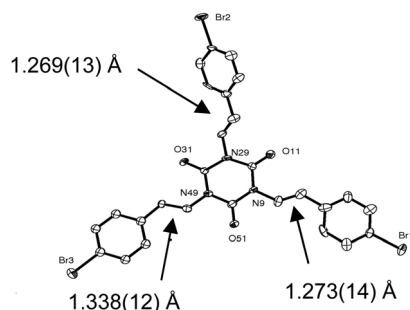


Fig. 1 ORTEP representation of **4-Br** at the 50% probability level with selected bond lengths indicated. Hydrogen atoms have been omitted for clarity.

The new compound **4-Br** was characterized by the usual techniques and by X-ray diffraction,<sup>‡</sup> providing definitive structural evidence for this intermediate (Fig. 1). In line with this solid-state structure, the <sup>1</sup>H NMR spectrum reveals the presence of only one isomer in solution with the classic AB pattern of *trans*-substituted double bonds in an *E* configuration (<sup>3</sup>*J*<sub>HH</sub> = 14.8 Hz). A striking difference with the triaryl isocyanurate derivatives previously crystallized is the overall coplanarity between the peripheral double bonds and the central heterocycle. One branch of the three presents a dihedral angle of *ca.* 45°, whereas the two others are nearly coplanar with dihedral angles of *ca.* 5° and 10°. This enforced coplanarity is certainly driven by the weak intramolecular hydrogen bonding existing between the carbonyl groups and the α- and β-hydrogen atoms on the *trans*-alkenyl spacers (and resulting in intramolecular O...H distances < 2.50 Å).

The extended derivative **3-NPh<sub>2</sub>** was then obtained in modest yield (18%) from **4-Br** by a Sonogashira coupling (Scheme 3), and was also fully characterized by the usual means. The presence of additional 1,4-phenylene-ethynylene units in the arms is clearly established by <sup>1</sup>H and <sup>13</sup>C NMR spectroscopy, and also by IR spectroscopy (ν<sub>C≡C</sub> at 2205 cm<sup>-1</sup>).

The enforced planarity of these two new tristyryl derivatives relative to their known triaryl analogues is confirmed by the DFT optimizations of these compounds. In CH<sub>2</sub>Cl<sub>2</sub>, a fully symmetric C<sub>3h</sub> structure is often slightly less stable than one with a tilted arm (C<sub>s</sub> symmetry), whereas they have nearly the same energy in vacuum. This can be explained by the fact that the dipole moment of the fully symmetric (C<sub>3</sub>) structure is close to zero, so the compound is not stabilized at all by the surrounding dielectric, in contrast to the C<sub>s</sub> structure which presents a non-zero

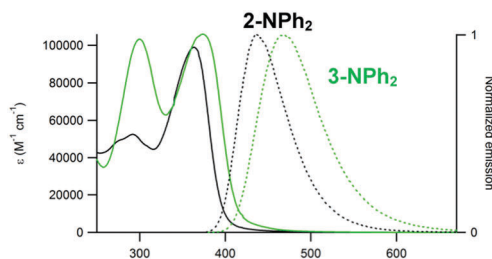


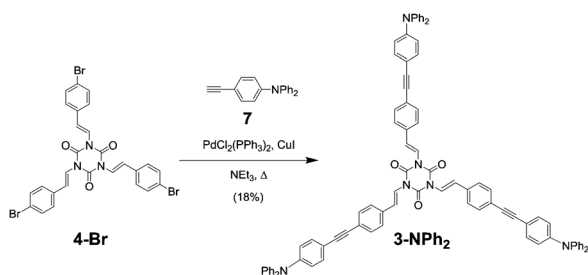
Fig. 2 Absorption and normalized emission spectra of **2-NPh<sub>2</sub>** (black) and **3-NPh<sub>2</sub>** (green) in CH<sub>2</sub>Cl<sub>2</sub> (20 °C).

dipole moment. The relative weakness of this stabilization means that several rotamers are likely to co-exist in solution, while no π-stacking could be evidenced experimentally by absorption spectroscopy (ESI<sup>†</sup>).

The UV-visible absorption and emission spectra of **4-Br** and **3-NPh<sub>2</sub>** were subsequently recorded. When compared to their corresponding analogues without a double bond in each arm (*i.e.* **1-Br** and **2-NPh<sub>2</sub>**), their first electronic transitions take place at slightly lower energies, in line with the extension and improved conjugation of their π-manifold. For instance, a 10 nm (*ca.* 735 cm<sup>-1</sup>) red-shift is seen for the first absorption of **3-NPh<sub>2</sub>** relative to that of **2-NPh<sub>2</sub>** (Fig. 2). While **4-Br**, similar to **1-Br** (Φ<sub>F</sub> = 0.0006), is nearly non-emissive in solution (Φ<sub>F</sub> = 0.0005), **3-NPh<sub>2</sub>** possesses a fluorescence quantum yield (Φ<sub>F</sub> = 0.61) slightly lower than that of **2-NPh<sub>2</sub>** (Φ<sub>F</sub> = 0.73), with again a red shift in emission (31 nm, *ca.* 1515 cm<sup>-1</sup>) that is attributable to the extension/planarization of the π-manifold in the former.

Similar to what had been previously established for **2-NPh<sub>2</sub>**,<sup>9</sup> DFT calculations confirm that the first electronic transition in **3-NPh<sub>2</sub>** corresponds to a LUMO/LUMO+1 ← HOMO/HOMO-1 (π-π\*) transition, implying some charge-transfer (CT) from the electron-rich periphery toward the central isocyanurate core (Fig. 3). According to DFT (see ESI<sup>†</sup>), this charge-transfer on the central ring is however less pronounced than in the shorter derivative **4-NPh<sub>2</sub>**. The shift to lower energy and the increase in transition moment when progressing from **2-NPh<sub>2</sub>** to **3-NPh<sub>2</sub>** are qualitatively confirmed by TD-DFT simulations (ESI<sup>†</sup>).

We then determined the two-photon absorption (2PA) of **3-NPh<sub>2</sub>** in the near-infrared (NIR) range (700–1000 nm) by investigating its two-photon excited fluorescence (TPEF) behavior. Contrary to our expectations based on previous examples,<sup>10</sup> it possesses a maximum 2PA cross-section of similar magnitude (*ca.* 410 GM),



Scheme 3 Synthesis of **3-NPh<sub>2</sub>**.

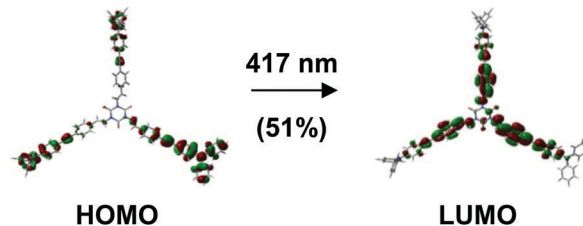


Fig. 3 Plots of the frontier molecular orbitals for **3-NPh<sub>2</sub>** primarily involved in the main excitation underlying the first allowed transition. Contour values are ±0.03 (e Bohr<sup>-3/2</sup>).

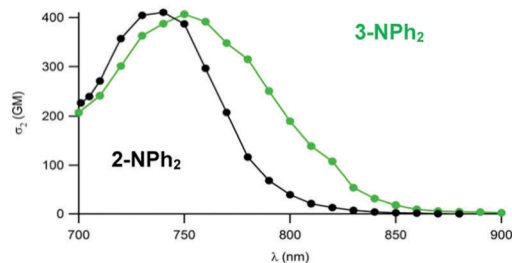


Fig. 4 Two-photon absorption spectra of **2-NPh<sub>2</sub>** and **3-NPh<sub>2</sub>** in dichloromethane (20 °C) in the near-IR range.

but slightly bathochromically-shifted and broadened compared to that of its non-styryl analogue **2-NPh<sub>2</sub>** (Fig. 4). The comparison of this band with its rescaled one-photon spectrum shows that, analogous to **2-NPh<sub>2</sub>** and in spite of the octupolar symmetry,<sup>11</sup> the 2PA takes essentially place in the first allowed 1PA excited state (see ESI†).

## Conclusions

This work reports the synthesis, full characterization and study of two new tristyryl isocyanurates **4-Br** and **3-NPh<sub>2</sub>**, the latter being an extended version of **2-NPh<sub>2</sub>**, the corresponding triphenyl analogue presenting remarkable two-photon absorption properties. As indicated by X-ray structural data, electronic spectroscopy and DFT calculations, the structure of **3-NPh<sub>2</sub>** allows now for better conjugation between the three donor groups and the central isocyanurate core through the  $\pi$ -manifold of the peripheral arms. However, in spite of these changes, this new octupole (**3-NPh<sub>2</sub>**) does not present a higher two-photon absorption cross-section than that of **2-NPh<sub>2</sub>**, at odds with what happened for related examples cited in the literature. This unexpected (and currently unexplained) statement warrants now further studies of these tristyryl isocyanurate derivatives to definitively settle that point and to understand better the origin of that rather uncommon phenomenon. However, on the practical side, the broader 2PA band found for **3-NPh<sub>2</sub>** will allow excitation to be performed further in the near-IR range.

## Experimental

The reactions were carried out under an inert atmosphere using Schlenk techniques. Solvents were freshly distilled under argon using standard procedures. The 3-(4-bromophenyl)-acryloyl azide **6-Br** and the 4-ethynyl-*N,N*-diphenylaniline **7** are known compounds (see ESI† for further details).<sup>13</sup>

### 1,3,5-Tri(4-bromostyryl)-1,3,5-triazinane-2,4,6-trione (**4-Br**).

A solution of 3-(4-bromophenyl)acryloyl azide (**6-Br**; 4.32 g, 17.1 mmol) in anhydrous toluene (20 mL) was heated at 68 °C. To measure the progress of the reaction, tubing was attached to the top of the condenser, and connected to an inverted test tube filled with water, to collect the volume of nitrogen evolved during the reaction. After completion of the reaction (12 h) the solvent was

evaporated under reduced pressure to yield the crude isocyanate (**5-Br**). The latter was then solubilized in nitrobenzene (8.50 mL) and 2 mol% of cesium fluoride (33 mg, 0.21 mmol) was added. The reaction mixture was stirred 48 h at room temperature giving in some cases a pale precipitate. A mixture of diethyl ether/hexane (1/1) was then added and the crude solid that formed was collected by filtration on a sintered glass filter funnel, before being purified by flash chromatography on silica gel ( $\text{CH}_2\text{Cl}_2$ /heptane = 1 : 1, v/v). Yield: 3.10 g (81%). HRMS (EI):  $m/z$  = 669.8971 [ $\text{M} + \text{H}$ ]<sup>+</sup> (calc. for  $\text{C}_{27}\text{H}_{19}\text{Br}_3\text{N}_3\text{O}_3$ : 669.8971). IR (neat):  $\nu$  = 1760 (C=O, vw), 1704 (C=O, s), 1655 (C=C, w). Raman (neat):  $\nu$  = 1764 (C=O, m), 1705 (C=O, vw), 1649 (C=C, vs). <sup>1</sup>H NMR (300 MHz, DMSO-*d*<sub>6</sub>)  $\delta$  = 7.59 (d,  $J$  = 8.7 Hz, 6H), 7.51 (d,  $J$  = 8.7 Hz, 6H), 7.15 (s, 6H, C=CH). <sup>13</sup>C NMR (75 MHz, DMSO-*d*<sub>6</sub>)  $\delta$  = 147.5, 134.4, 132.3, 129.0, 127.8, 121.8, 121.5. X-ray-quality crystals were grown by slow diffusion of pentane into a  $\text{CDCl}_3$  solution of **4-Br**.

### 1,3,5-Tri(4-((4-(diphenylamino)phenyl)ethynyl)styryl)-1,3,5-triazinane-2,4,6-trione (**3-NPh<sub>2</sub>**)

1,3,5-Tri((*E*)-4-bromostyryl)-1,3,5-triazinane-2,4,6-trione (**4-Br**; 0.237 g, 0.35 mmol) and 4-ethynyl-*N,N*-diphenylaniline (**7**; 0.426 g, 1.58 mmol) were introduced into a flask under argon. Deoxygenated triethylamine (2.5 mL) was added, and then copper iodide (8.30 mg, 43.6  $\mu\text{mol}$ ) and bis(triphenylphosphine)palladium(II) dichloride (15.20 mg, 21.60  $\mu\text{mol}$ ). The reaction was heated at 85 °C for 20 h. After cooling to room temperature, the mixture was filtered through a pad of celite and the filtrate evaporated to dryness. The crude product was purified by column chromatography (silica gel,  $\text{CH}_2\text{Cl}_2$ /heptane = 70 : 30, v/v). A dark yellow-green compound was obtained. Yield: 80 mg (18%). HRMS (EI):  $m/z$  = 1236.4706 [ $\text{M}$ ]<sup>+</sup> (calc. for  $\text{C}_{87}\text{H}_{60}\text{N}_6\text{O}_3$ : 1236.4721). IR (neat):  $\nu$  = 2204 (C $\equiv$ C, m), 1772 (C=O, vw), 1707 (C=O, s), 1653 (sh, C=C, w). <sup>1</sup>H NMR (300 MHz,  $\text{CDCl}_3$ ):  $\delta$  = 7.52 (d,  $J$  = 8.4 Hz, 6H), 7.44 (d,  $J$  = 8.4 Hz, 6H), 7.40 (d,  $J$  = 8.6 Hz, 6H), 7.33 (d,  $J$  = 14.8 Hz, 3H), 7.34–7.27 (m, 12H), 7.21 (d,  $J$  = 14.8 Hz, 3H), 7.16–7.12 (m, 12H), 7.12–7.06 (m, 6H), 7.03 (d,  $J$  = 8.6 Hz, 6H). <sup>13</sup>C NMR (75 MHz,  $\text{CDCl}_3$ ):  $\delta$  = 148.0, 147.2, 146.5, 134.2, 132.6, 131.8, 129.4, 128.6, 126.6, 125.0, 123.8, 123.6, 122.2, 119.7, 115.9, 91.1, 88.5.

### Luminescence measurements

Luminescence measurements in solution were performed in dilute air-equilibrated solutions contained in quartz cells of 1 cm pathlength (*ca.*  $10^{-6}$  M, optical density < 0.1) at room temperature (20 °C), using an Edinburgh Instruments (FLS920) fluorimeter in photon-counting mode. Luminescence quantum yields were measured according to literature procedures.<sup>14,15</sup>

### Two-photon excited fluorescence measurements

TPEF cross-sections were measured relative to fluorescein in 0.01 M aqueous NaOH<sup>16</sup> using the well-established method described by Xu and Webb<sup>17</sup> and the appropriate solvent-related refractive index corrections.<sup>18</sup> Reference values between 700 and 715 nm for fluorescein were taken from the literature.<sup>19</sup> The quadratic dependence of the fluorescence intensity on the excitation power was checked for each sample and all wavelengths. A Chameleon Ultra II (Coherent) laser was used, generating 140 fs pulses at a

80 MHz repetition rate. The excitation was focused into the cuvette through a microscope objective (10 $\times$ , NA 0.25). The fluorescence was detected in epifluorescence mode *via* a dichroic mirror (Chroma 675dxcru) and a barrier filter (Chroma e650sp-2p) by a compact CCD spectrometer module BWTek BTC112E. Total fluorescence intensities were obtained by integrating the corrected emission.

### X-ray crystallography

Data collection of crystals of **4-Br** was performed on a D8 VENTURE AXS diffractometer at 150 K, with graphite monochromatized MoK $\alpha$  radiation. The structure was solved by direct methods using the SIR97 program<sup>20</sup> and subsequently refined with full-matrix least-square methods based on  $F^2$  (SHELXL-97).<sup>21</sup> The contribution of the disordered solvents to the calculated structure factors was estimated following the BYPASS algorithm,<sup>22</sup> implemented as the SQUEEZE option in PLATON.<sup>23</sup> A new data set, free of solvent contribution, was then used in the final refinement. All non-hydrogen atoms were refined with anisotropic atomic displacement parameters. H atoms were included in the final cycle of refinement in their calculated positions. A final refinement on  $F^2$  with 6191 unique intensities and 295 parameters converged at  $\omega R(F^2) = 0.1884$  ( $R(F) = 0.0978$ ) for 4555 observed reflections with  $I > 2\sigma(I)$ . The data have been deposited at the Cambridge Crystallographic Data Centre (CCDC 1511480).<sup>†</sup>

### Computational details

The DFT calculations reported in this work have been performed using the Gaussian09<sup>24</sup> program. The geometries of all the compounds have been optimized without symmetry constraints using the MPW1PW91 functional<sup>25</sup> and the 6-31G\* basis set. The solvent effects were taken into account (Polarizable Continuum Model).<sup>26</sup> Calculation of the frequencies of normal modes of vibration were carried out to confirm the true minima character of the optimized geometries. TD-DFT calculations were performed at the same level of theory using the previously optimized geometries. Swizard<sup>27,28</sup> was used for plotting the simulated spectra and GaussView<sup>29</sup> was employed for the MO plots.

### Conflicts of interest

There are no conflicts of interest to declare.

### Acknowledgements

The CNRS (PICS program No. 7106 and LIA No. 1194) and ANR (Isogate Project) are acknowledged for financial support. O. M. and A. T. thank the Region Bretagne for a PhD grant. M. G. H. thanks the Australian Research Council (ARC) for financial support. We acknowledge the HPC resources of CINES and of IDRIS under the allocations 2016-[x2015080649] and 2017-[x2016080649] made by GENCI (Grand Equipement National

de Calcul Intensif). We also wish to thank Hugo Coupevent and Axel Lehmann for assistance in the synthesis.

### Notes and references

<sup>†</sup> Crystal data: C<sub>27</sub>H<sub>18</sub>Br<sub>3</sub>N<sub>3</sub>O<sub>3</sub>,  $M = 672.17$ , monoclinic, space group  $P2_1/n$ ,  $a = 19.931(3)$  Å,  $b = 6.4376(9)$  Å,  $c = 21.314(3)$  Å,  $U = 2684.8(6)$  Å<sup>3</sup>,  $Z = 4$ ,  $R = 0.0978$  (see ESI<sup>†</sup> for details).

- 1 B. R. Cho, K. H. Son, S. H. Lee, Y. S. Song, Y. K. Lee, S. J. Jeon, J. H. Choi, H. Lee and M. Cho, *J. Am. Chem. Soc.*, 2001, **123**, 9412–9417.
- 2 W. H. Lee, S. H. Lee, J.-A. Kim, J. H. Choi, M. Cho, S.-J. Jeon and B. R. Cho, *J. Am. Chem. Soc.*, 2001, **123**, 10658–10667.
- 3 F. Terenziani, C. Katan, E. Badaeva, S. Tretiak and M. Blanchard-Desce, *Adv. Mater.*, 2008, **20**, 4641–4678.
- 4 G. S. He, L.-S. Tan, Q. Zheng and P. N. Prasad, *Chem. Rev.*, 2008, **108**, 1245–1330.
- 5 H. M. Kim and B. R. Cho, *Chem. Commun.*, 2009, 153–164.
- 6 R. G. Arnold, J. A. Nelson and J. J. Verbanc, *Chem. Rev.*, 1957, **57**, 47–76.
- 7 H. Ulrich, *The Chemistry and Technology of Isocyanates*, J. Wiley & Sons, New York, 1996.
- 8 G. Argouarch, R. Veillard, T. Roisnel, A. Amar, A. Boucekkine, A. Singh, I. Ledoux and F. Paul, *New J. Chem.*, 2011, **35**, 2409–2411.
- 9 G. Argouarch, R. Veillard, T. Roisnel, A. Amar, H. Meghezzi, A. Boucekkine, V. Hugues, O. Mongin, M. Blanchard-Desce and F. Paul, *Chem. – Eur. J.*, 2012, **18**, 11811–11826.
- 10 Y. Z. Cui, Q. Fang, G. Xue, G. B. Xu, L. Yin and W. T. Yu, *Chem. Lett.*, 2005, **34**, 644–645.
- 11 J. C. Collings, S.-Y. Poon, C. Le Droumaguet, M. Charlot, C. Katan, L.-O. Pålsson, A. Beeby, J. A. Mosely, H. M. Kaiser, D. Kaufmann, W.-Y. Wong, M. Blanchard-Desce and T. B. Marder, *Chem. – Eur. J.*, 2009, **15**, 198–208.
- 12 C. Irle and W. Mormann, *Liq. Cryst.*, 1996, **21**, 295–305.
- 13 T. Terai, M. Kohno, G. Boncompain, S. Sugiyama, N. Saito, R. Fujikake, T. Ueno, T. Komatsu, K. Hanaoka, T. Okabe, Y. Urano, F. Perez and T. Nagano, *J. Am. Chem. Soc.*, 2015, **137**, 10464–10467.
- 14 N. Demas and G. A. Crosby, *J. Phys. Chem.*, 1971, **75**, 991–1024.
- 15 G. R. Eaton, *Pure Appl. Chem.*, 1988, **60**, 1107–1114.
- 16 M. A. Albota, C. Xu and W. W. Webb, *Appl. Opt.*, 1998, **37**, 7352–7356.
- 17 C. Xu and W. W. Webb, *J. Opt. Soc. Am. B*, 1996, **13**, 481–491.
- 18 M. H. V. Werts, N. Nerambourg, D. Pélégry, Y. Le Grand and M. Blanchard-Desce, *Photochem. Photobiol. Sci.*, 2005, **4**, 531–538.
- 19 C. Katan, S. Tretiak, M. H. V. Werts, A. J. Bain, R. J. Marsh, N. Leonczek, N. Nicolaou, E. Badaeva, O. Mongin and M. Blanchard-Desce, *J. Phys. Chem. B*, 2007, **111**, 9468–9483.
- 20 A. Altomare, M. C. Burla, M. Camalli, G. Cascarano, C. Giacovazzo, A. Guagliardi, A. G. G. Moliterni, G. Polidori and R. Spagna, *J. Appl. Crystallogr.*, 1999, **32**, 115–119.
- 21 G. M. Sheldrick, *Acta Crystallogr., Sect. A: Found. Crystallogr.*, 2008, **64**, 112–122.

- 22 P. v. d. Sluis and A. L. Spek, *Acta Crystallogr.*, 1990, **A46**, 194–201.
- 23 A. L. Spek, *Appl. Crystallogr.*, 2003, **36**, 7–13.
- 24 M. J. Frisch, *et al.*, *Gaussian09*, 2015.
- 25 C. Adamo and V. Barone, *J. Chem. Phys.*, 1998, **108**, 664–675.
- 26 J. Tomasi, B. Mennucci and R. Cammi, *Chem. Rev.*, 2005, **105**, 2999–3093.
- 27 S. I. Gorelsky, *SWizard program, Revision 4.5*, 2013.
- 28 S. I. Gorelsky and A. B. P. Lever, *J. Organomet. Chem.*, 2001, **635**, 187–196.
- 29 R. Dennington, T. Keith and J. Millam, *GaussView version 5*, 2003.